JOURNAL OF MATERIALS SCIENCE (1998) 3607–3614

Effect of fabrication parameters on the microstructural quality of fibre–foil titanium metal matrix composites

M. P. THOMAS*, J. G. ROBERTSON†, M. R. WINSTONE*
Structural Materials Centre, Defence Evaluation, and Research Agency, Ively Road, Farnborough, Hants. GU14 OLX, UK and † DERA Sigma, Defence Evaluation and Research Agency, RAE Road, Farnborough, Hants. GU14 6XE, UK

The microstructure of fibre–foil Ti–6Al–4V (composition in weight per cent) and IMI 834 matrix metal matrix composites (MMCs), and corresponding foil-bonded alloys, are investigated in relation to fabrication parameters. Higher fabrication temperatures are required in IMI 834 MMCs, which results in a thicker interfacial reaction layer than in Ti–6Al–4V MMCs. The matrix microstructure in all materials is predominantly α with intergranular β, as a result of the slow cooling rate. MMCs reinforced with SM1240 fibres exhibit boron precipitates along foil bond lines, owing to diffusion during consolidation. Fabrication using fibre mats with 7.1 fibres per millimeter (FPM) results in an excellent microstructure in (Ti–6Al–4V)–SM1240. The larger diameter of the SM1140 + fibre compared with SM1240 means that (Ti–6Al–4V)–SM1140 + requires FPM significantly below 7.1 in order to produce acceptable microstructural quality. The higher residual stresses in IMI 834 MMCs result in cracking of the matrix and fibre–matrix interfacial region when a FPM of 7.1 is used. Acceptable microstructural quality is observed in IMI 834 MMCs when the FPM of fibre mats is reduced to 6.3. Interfibre cracking in IMI 834–SM1140 + is enhanced by a higher matrix microhardness than the other materials. This high hardness may be caused by a high matrix carbon content. © *1997 British Crown*

1. Introduction

The improved thrust-to-weight ratios expected of the next generation of aeronautical gas-turbine engines has necessitated the development of "step-change" materials which offer improved specific mechanical properties and higher temperature capabilities than those currently used. SiC-fibre-reinforced titanium (Ti) metal matrix composites (MMCs) are generating much interest for use in gas turbines because they exhibit improved specific strength and stiffness and better creep and fatigue resistance than monolithic Ti alloys do, when the stress is along the fibre axis. They also maintain good mechanical properties to temperatures at which monolithic Ti alloys cannot be used. They have been identified as "key materials" for the future of the aerospace industry by the UK Materials Strategy Commission, in their Technology Foresight Programme [1]. In the USA, the Integrated High Performance Turbine Engine Technology Programme (IHPTET) also regards Ti MMCs as being of prime importance and has a research consortium dedicated to this material [2].

The Structural Materials Centre of the Defence Evaluation and Research Agency is manufacturing and studying Ti MMCs for potential use in aeronautical gas-turbine components. It has been noted in this programme that microstructural features present in the MMCs, in the as-received condition, can effect their mechanical performance. An appreciation is required, therefore, of how the fabrication process can affect microstructural quality. This paper investigates the effect on the microstructure of the materials' thermal history, and the fibre per millimetre (FPM) value used during filament winding of fibre mats.

2. Materials and procedure

Four Ti MMCs are being studied. They consist of either a Ti–6Al–4V matrix (composition in weight per cent) or an IMI 834 (Ti–5.8Al–4.0Sn–3.5Zr–0.7Nb–0.5Mo–0.35Si–0.06C) matrix (composition in weight per cent) reinforced with SM1140 + or SM1240 fibres. The SM1140 + fibre is a tungsten-cored SiC fibre of 100 μm diameter produced by chemical

vapour deposition (CVD), with a 5 μm surface carbon layer. SM1240 is a tungsten-cored of CVD SiC fibre 100 μm diameter with a 1.3 μm carbon coating followed by an outer 1.3μm of TiB_x. This outer layer consists of TiB_2 crystals embedded in a free B matrix.

Six panels of each MMC were produced via the fibre–foil route, with a nominal fibre volume fraction of 0.33. Panel thickness was either six ply (approximately 1 mm) or eight ply (approximately 1.3 mm). The MMC fabrication process has been detailed previously [3]. Two unreinforced panels of each matrix alloy were manufactured from alloy foils using the same fabrication parameters as the MMCs, to act as a control.

The spacing of fibres in consolidated MMCs is dictated by the quality of fibre management during production of the fibre mats, by the FPM value used during fibre mat production and by the thickness of the matrix foils. Poor fibre management can lead to touching fibres and longitudinal fibre bending, whatever FPM value is used. Where consistent, high-quality fibre management is employed, however, the FPM value and the matrix foil thickness become the dominant factor in fibre spacing and are the primary means by which fibre volume fractions are varied between MMC panels. The current work focuses on the effect of the FPM value on the microstructural quality. The thickness of matrix foils has been controlled, where necessary, using a $HF–HNO_3$ etchant to achieve nominally the same fibre volume fraction in all panels. All panels of (Ti–6Al-4V)–SM1240 were manufactured with a FPM of 7.1, which has been successfully used as standard for this MMC for several years. The other MMCs were fabricated with a range of FPM values.

Specimens were taken at least 10 mm inside the panels in order to avoid edge defects. Wavelength-dispersive X-ray (WDX) line scans were conducted through the matrix between two fibres in neighbouring plies (approximate line scan length, 50 μm). The line scans were conducted between fibres in neighbouring plies, rather than neighbouring fibres in the same ply, so as to avoid any debris occurring along foil bond lines. Similar length line scans were conducted in the foil-bonded alloys. A JEOL Superprobe JXA-8600 was used, with an acceleration voltage of 10 kV and beam current of approximately 16 nA. WDX line scans were also conducted along foil bond-lines to identify precipitates observed in this location.

Microhardness measurements were made on all panels in the unetched condition, using a load of 300 g, application time of 15 s and a Vickers-type indenter in accordance with [4]. For the MMCs, microhardness measurements were taken in the matrix, as far away from fibres and foil bond lines as possible. Six readings were taken for each panel, and the mean and standard deviation of the most consistent five readings were calculated.

After conducting the above analysis, specimens were etched in Kroll's reagent and examined in an optical photo microscope.

3. Results and discussion

3.1. Fibres and interfaces

The fibre distribution is good for all the MMCs, with generally consistent fibre spacing and no longitudinal fibre bending, which can cause problems in Ti MMCs [5]. Fig. 1 shows the example of (Ti–6A1–4V)–SM1240. In all panels the fibre packing is a mixture of square and hexagonal as shown in Fig. 2.

In all the MMCs, neighbouring fibres within a ply were occasionally touching (arrowed in Fig. 2). Panels of (Ti–6Al–4V)–SM1240 show little presence of touching fibres, confirming that a FPM of 7.1 is satisfactory for this material. At the same FPM value, however, panels of (Ti–6Al–4V)–SM1140 + contain larger numbers of touching fibres. These effects are due to the larger diameter of the SM1140 + fibre compared with SM1240. Reducing the FPM to 6.2 successfully reduces the number of touching fibres to the level seen in (Ti–6Al–4V)–SM1240.

In both IMI 834 MMCs, a FPM of 7.1 results in relatively high numbers of touching fibre pairs. Reducing the FPM is successful in reducing the amount of touching fibres. From Fig. 3 it is seen that, for IMI 834 MMCs, a FPM of less than 6.3 is required to reduce the number of touching fibre pairs per thousand fibres to the level seen in (Ti–6Al–4V)–SM1240.

Touching fibres will have little or no bond between them and therefore form a linear discontinuity in the MMC. Such a defect will be most deleterious where

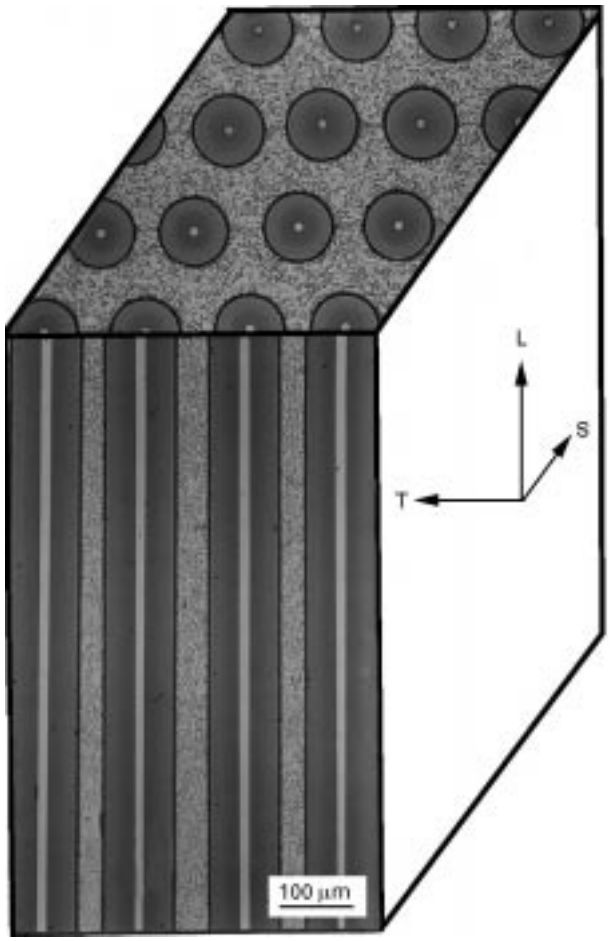

Figure 1 Microstructure of (Ti–6Al–4V)–SM1240 Ti MMC. All other MMCs are similar.

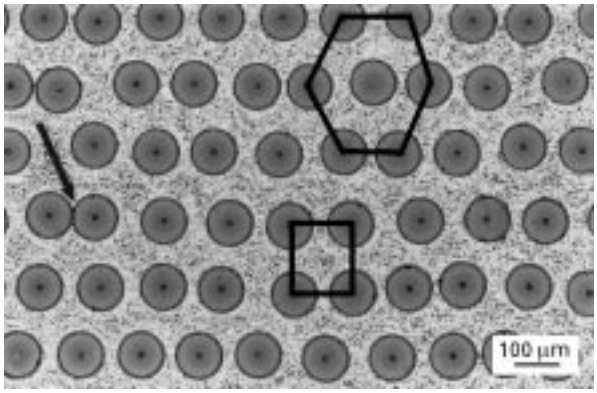

Figure 2 Variability of packing arrangement in the MMCs. IMI 834–SM1140 + Ti MMC is shown, but the arrangement is seen in all four MMCs. Note the touching fibres (arrowed).

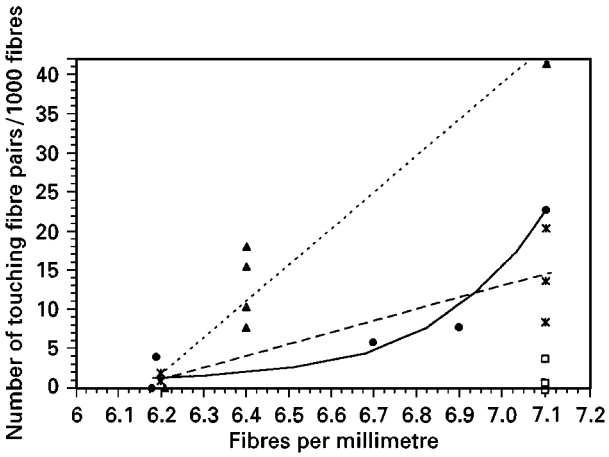

Figure 3 The number of touching fibre pairs per 1000 fibres as a function of the FPM value. (——), (∗) IMI 318–SM1140 + ; (□) IMI 318–SM1240, (- - -), (▲), IMI 834–SM1140 + ; (—), (●), IMI 834–SM1240.

stress is applied normal to this discontinuity (i.e., in transverse specimens).

The chemistry of interfacial reaction has been well characterized in Ti MMCs reinforced with both carbon-coated and C–TiB_x-coated SiC fibres and need not be discussed here. It is apparent from Fig. 4 that greater interfacial reaction has occurred in IMI 834 MMCs than in Ti–6Al–4V MMCs. This is particularly apparent in the SM1240 fibre-reinforced materials, where the TiB_2–TiB reaction layer is approximately 0.5 μm thick in (Ti–6Al–4V)–SM1240 but over 1.5 μm thick in IMI 834–SM1240 (compare Fig. 4b and d). This is due to the higher temperature required to consolidate IMI 834 MMCs fully. As a result, the fabrication process for IMI 834 MMCs has been optimized to minimize interfacial reaction.

Cracking of the fibre coatings and interfacial reaction products is rarely observed in Ti–6Al–4V MMCs. In IMI 834–SM1140 +, small amounts of carbon coating cracking were observed between closely spaced fibres in the panel with a FPM of 7.1. At lower FPM values no coating or interfacial cracking is observed. In IMI 834–SM1240 extensive cracking of the TiB_2–TiB reaction layer occurs between neighbouring fibres in the same ply, in the panel with a FPM of 7.1

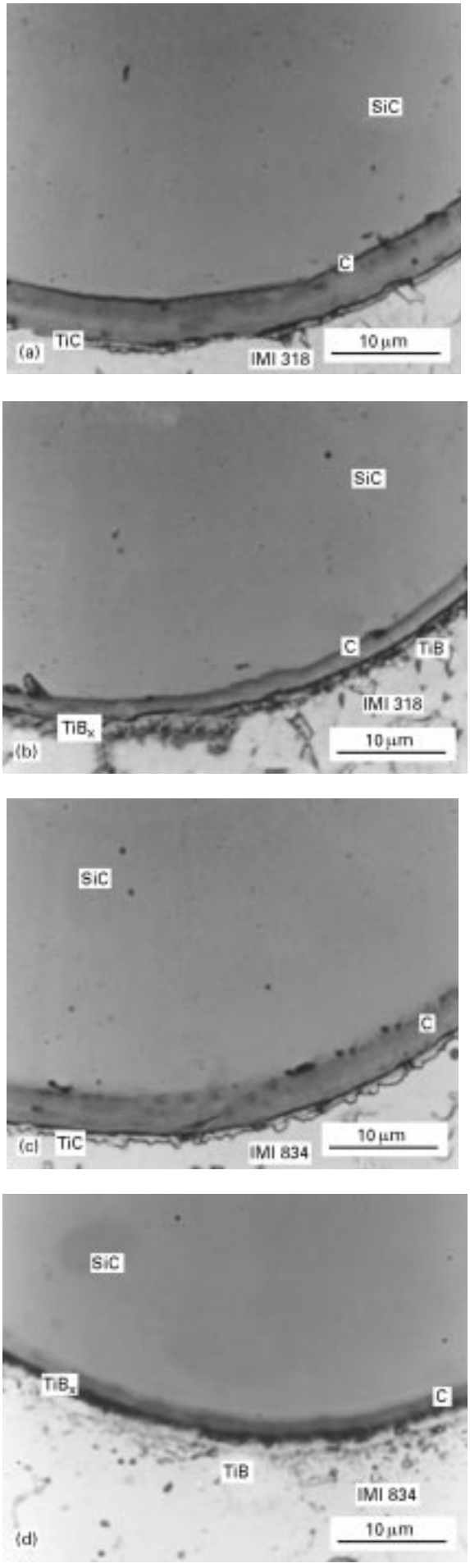

Figure 4 Interfacial reaction layers in the MMCs: (a) (Ti–6Al–4V)–SM1140 + ; (b) (Ti–6Al–4V–SM1240; (c) IMI 834–SM1140 + ; (d) IMI 834–SM1240.

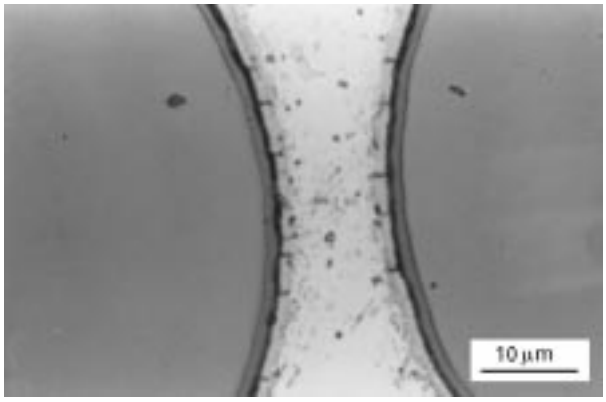

Figure 5 Cracking of the TiB_2–TiB reaction layer in panel C19 of IMI 834–SM1240. Fibre coating and interfacial cracking are occasionally seen in all MMCs.

(Fig. 5). This reaction layer cracking, which has been witnessed in other Ti MMCs [5–8], results from the high residual tensile hoop stresses [5, 8] generated by the close spacing of fibres. When the FPM is lowered to 6.9, the cracking is much reduced and, in all panels of IMI 834–SM1240 with a FPM of 6.2, the interfacial cracking is eradicated completely. The interfacial cracking may have a deleterious effect on the mechanical properties along the *S* axis (i.e., in through-thickness specimens), as they will act as stress concentrators.

3.2. Matrices

Fig. 6 shows the microstructure of the foil-bonded Ti–6Al–4V. The microstructure of the matrices in the Ti–6Al–4V MMCs were identical. The microstructure consists of equiaxed α phase with small amounts of intergranular β phase. WDX line scans indicate that the β phase is deficient in aluminium, but rich in vanadium. The α-dominated microstructure and partitioning of α-stabilizing aluminium and β-stabilizing vanadium result from the maximum temperature of the fabrication cycle, being significantly below that used to solution conventional α + β-Ti alloys. The upper temperature used in the fibre–foil fabrication process is limited by the need to prevent excessive interfacial reaction. The low cooling rate from the fabrication temperature, necessary to limit residual stresses, will also contribute to the observed microstructure [9]. It is noted that, although this matrix microstructure is likely to provide good fracture toughness [10], a bimodal microstructure will significantly enhance the tensile strength and fatigue resistance [10–13].

In all the Ti–6Al–4V-based materials the α grain size is of the order of 10 μm which is typical of a wide range of Ti MMCs (e.g., [14]). WDX line scans of the Ti–6Al–4V MMCs show a higher carbon content than in the foil-bonded Ti–6Al–4V, but the standard deviation of data means that this was not significant. Margins of error are large, however, and (Ti–6Al–4V)–SM1140 + might be expected to have a high carbon content in the matrix because of carbon diffusion from the fibre coating during consolidation.

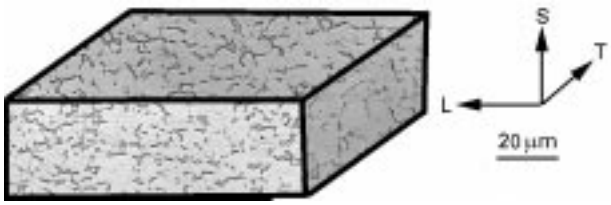

Figure 6 Microstructure of Ti alloy in Ti–6Al–4V-based materials. (Ti–6Al–4V)–SM1140+ MMC is shown, but all the others are similar.

A previous study noted a shift in the β transus approach curve to higher temperatures in Ti–6Al–4V MMCs compared with monolithic Ti–6Al–4V [15]. This was attributed to the fact that greater amounts of α-stabilizing elements are present in the MMC matrices, most probably carbon which diffused from the fibre coating during MMC fabrication. In that study the β transus approach curve of (Ti–6Al–4V)–SM1140 + shifted to higher temperatures than that for (Ti–6Al–4V)–SM1240, suggesting that the relative carbon contents for the materials increased in the order Ti–6Al–4V, (Ti–6Al-4V)–SM1240, (Ti–6Al–4V)–SM1140 + , which would logically be expected if the carbon was originating from the fibre coatings.

(Ti–6Al–4V)–SM1240 displays fine stringers of precipitates along approximately 40% of prior foil-bond lines (Fig. 7). WDX line scans show that these precipitates are rich in boron and rarely occur in the matrix away from foil bond lines (Fig. 8). No other elements exhibit peaks at these points, suggesting that the precipitates are Ti borides. Foil bond-line precipitates have occasionally been observed in previous studies. In one case, large precipitates on the foil bond lines in an SCS-6-fibre-reinforced Ti–15V–3Cr–3Al–3Sn alloy were attributed to pieces of interfacial reaction zone breaking away from the fibre–matrix interface during consolidation and being pushed into the matrix [7]. Investigation of the fibre–foil consolidation process, however, suggests that such a mechanism is unlikely, because of the creep directions of the matrix foils during consolidation [5, 6]. Reference to other literature shows that the foil bond-line precipitates in [7] consisted of TiC and were, in fact, the products of reaction between Ti cross-weave wires in the original fibre mats, and carbon that diffused into the matrix during fabrication [17, 18].

Investigation of the literature on boron and carbon diffusion in Ti alloys allows the following explanation to be proposed for the foil bond-line boride precipitates. The presence of boride precipitates in the matrices and on foil bond lines, but not carbides, arises most probably because boron has a higher diffusivity in Ti than carbon does [19–21], but a lower solubility [19, 22–24]. Diffusivity of any element increases when the diffusion route changes from bulk to grain boundaries to free surfaces [25]. For a given time, boron will diffuse a greater distance along foil surfaces than through grain boundaries or bulk matrix, as shown by the equation

$$x = \sqrt{(Dt)} \quad (1)$$

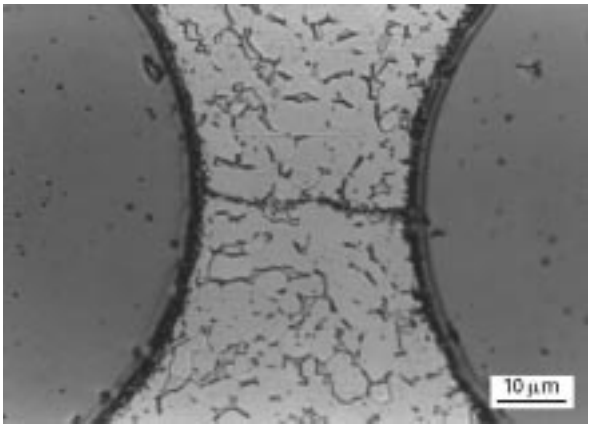

Figure 7 Precipitates on the foil bond line of (Ti–6Al–4V)–SM1240.

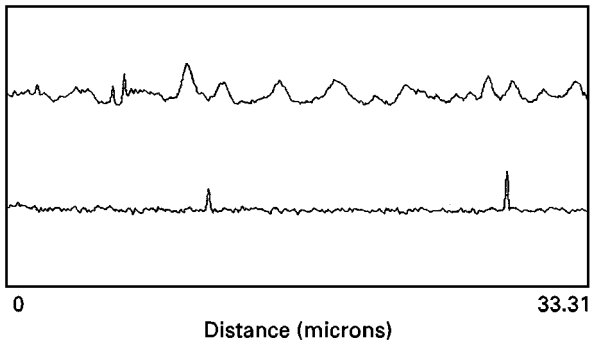

Figure 8 WDX line scans in (Ti–6Al–4V)–SM1240 (peaks indicate the presence of boron). Upper curve, from fibre to fibre, along the foil bond line in Fig. 7; lower curve, from fibre to fibre through the matrix away from the bond line in Fig. 7.

where x is the distance of diffusion, D the diffusivity and, t the time of diffusion. A corollary of this is that, for a fixed distance x from the fibre–matrix interface, the concentration of boron will be higher at the foil surface than at a distance x along grain boundaries or bulk matrix. A second consideration is that grain boundaries and free surfaces are areas where atoms can lower their free energies. Hence boron atoms are attracted to free surfaces and, to a lesser extent, to grain boundaries [25]. Grain-boundary triple points are likely to attract sufficient boron, through diffusion along multiple grain boundaries and through migration of bulk boron, to form precipitates during post-fabrication cool-down. It is these triple point precipitates that have been detected in the bulk scan of Fig. 8. The free surfaces of Ti foils will have a high concentration of boron, through diffusion along the free surfaces from the fibre coating and from migration of boron from nearby grain boundaries and bulk matrix. This boron concentration will be doubled when the free surfaces of neighbouring foils meet and bond together during the hot isostatic pressing process. Thus, during post-consolidation cool-down of the MMC, a large number of boron precipitates will form along the foil bond lines.

Borides are relatively brittle. The planes of titanium boride precipitates on foil bond lines may, therefore, have a deleterious effect on the mechanical properties of SM1240-fibre reinforced MMCs, where the applied stress is normal to the precipitate planes. Tests are currently under way to assess any such effect, made possible by the successful development of a through-thickness tensile specimen [26].

Fig. 9 shows the microstructure of the foil-bonded IMI 834. The matrices in the IMI 834 MMCs were identical. The microstructure is similar to that of the foil-bonded Ti–6Al–4V, with a predominantly α structure with small amounts of β at grain boundaries. The microstructure of the IMI 834 alloy and MMCs is not that required to give optimum mechanical performance as a result of the low temperatures used during MMC fabrication and the low cooling rate. A significant improvement in creep resistance, for instance, could be obtained by changing the microstructure to predominantly transformed β [27], without the fatigue performance being altered significantly. As with

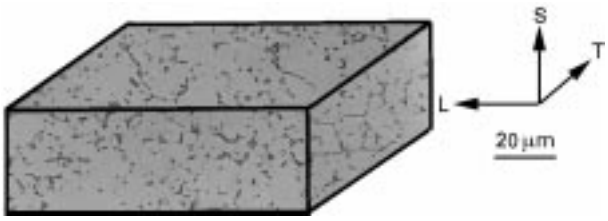

Figure 9 Microstructure of Ti alloy in IMI 834 materials. IMI 834–SM1140 + MMC is shown, but all the others are similar.

the Ti–6Al–4V alloy, the grain size in the IMI 834 alloy and matrices is approximately 10 μm. The main difference between the two Ti alloys is that the IMI 834 alloy and matrices exhibit large numbers of equiaxed precipitates with diameters of 1 μm or less (compare Figs 6 and 9). WDX line scans show these precipitates to be rich in Si and Zr and deficient in Al (Fig. 10). They are most likely to be the S_2 silicide ($(TiZr)_6Si_3$) often seen in IMI 834 alloy [28, 29], since the S_1 silicide is rarely observed in this alloy. Reference to the Ti–Si phase diagram for IMI 834 suggests that, at the fabrication temperature of the IMI 834 MMCs, silicide formation will occur [29, 30]. After consolidation, the IMI 834 materials are cooled to an intermediate temperature and held for a short time before cooling to room temperature. Extensive nucleation and growth of S_2 precipitates is known to occur when IMI 834 is aged at similar intermediate temperatures [28, 30]. The presence of the S_2 precipitates in the current IMI 834 materials is fully explained, therefore, by the thermal history of the materials. The number and size of these silicides do not change between the foil-bonded IMI 834 and the MMC matrices. The presence of silicide particles in IMI 834 alloy will reduce the ductility [31] and may also reduce the low cycle fatigue life [28].

The IMI 834 matrices show a higher carbon content than the foil-bonded alloy, although the standard deviation of WDX data suggests that this is not significant. A previous study, using Auger electron spectroscopy, has shown that whilst monolithic IMI 834 and IMI 834–SM1240 have similar carbon contents, the matrix in IMI 834–SM1140 + contains significantly more carbon [32].

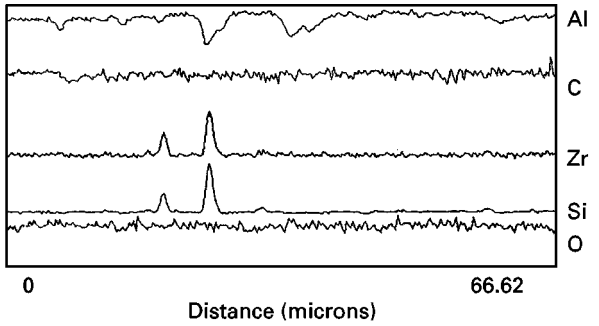

Figure 10 WDX line scans through foil-bonded IMI 834. Similar line scans are obtained for IMI 834–SM1140 + and IMI 834–SM1240.

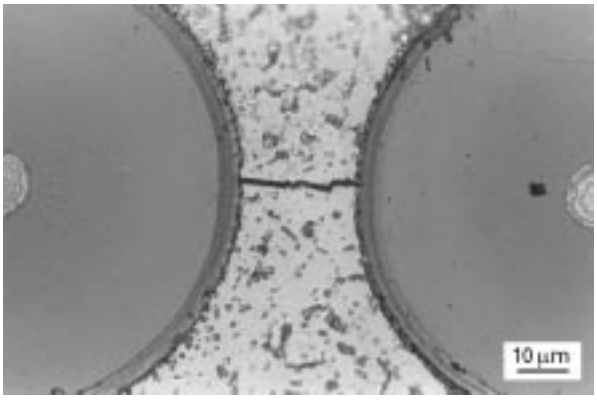

Figure 11 Interfibre cracking of the matrix in the IMI 834–SM1140 + . This is also occasionally seen in IMI 834–SM1240.

Boron-rich foil bond-line precipitates are seen in IMI 834–SM1240 as they are in (Ti–6Al–4V)–SM1240. The precipitates are more prevalent in the IMI 834 matrix, because of the higher fabrication temperature which leads to greater amounts of boron diffusion.

Significant interfibre matrix cracking occurs in panels of the IMI 834 MMCs with a FPM of 7.1. Such cracking is negligible in Ti–6Al–4V MMCs. The cracks initiate predominantly at the interfacial reaction zones and appear to pass preferentially through S_2 precipitates. The angular path of the cracks is indicative of transgranular cleavage (Fig. 11). IMI 834 has greater high-temperature strength than Ti–6Al–4V. Thermal mismatch stresses in IMI 834 MMCs will, therefore, become significant at a higher temperature than those in Ti–6Al–4V MMCs, and ambient-temperature residual stresses will be higher. The interfibre cracks occur only between closely spaced fibres in the outer plies, which is where the residual stresses are highest [6, 7, 33]. For a given FPM value, IMI 834 SM1140 + shows a greater propensity to matrix cracking than IMI 834 SM1240 does, which may be due in part to the larger fibre diameter of SM1140 +. For both IMI 834 MMCs reducing the FPM value reduces the number of matrix cracks (Fig. 12). As with the case of touching fibres (Fig. 3), a FPM of 6.3 or less is required to improve the structural quality of IMI 834 MMCs to a level seen in (Ti–6Al–4V)–SM1240.

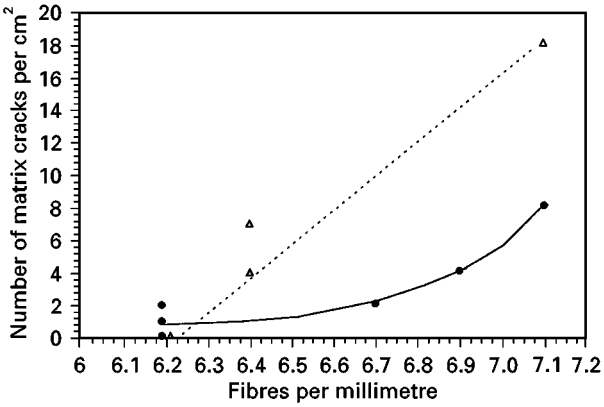

Figure 12 Propensity for interfibre matrix cracking as a function of the FPM value. (…), (△), IMI 834–SM1140 + ; (—), (●), IMI 834–SM1240.

Fig. 13 presents the results of the microhardness measurements. For each material there is no significant difference between the hardness of individual panels, indicating a consistent fabrication process. There is no significantly difference between the hardness of the three Ti–6Al–4V materials, indicating that impingement of fibres into the hardness-indentation deformation zone has not caused an increase in the measured hardness of the MMCs compared with the foil-bonded alloy. The hardness of the Ti–6Al–4V materials are similar to those previously reported [34]. Foil-bonded IMI 834 shows slightly greater hardness than Ti–6Al–4V, owing to increased solid-solution hardening and precipitation hardening. IMI 834–SM1240 does not show any significant difference in hardness from the foil-bonded alloy, but IMI 834–SM1140+ is significantly harder than all other

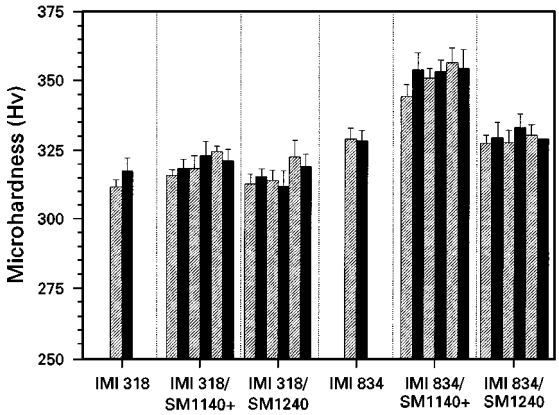

Figure 13 Microhardness measurements. Each column is the mean of the five most consistent readings from a series of six.

materials tested. The hardness of the matrix can be due to the effect of precipitation and the presence of interstitial elements. In the present case, the most likely explanation is the diffusion of carbon from the fibre coating, as suggested earlier. The matrix in IMI 834–SM1140+ would be expected to have a higher carbon content than (Ti–6Al–4V)–SM1140+, because of the higher fabrication temperature. A high carbon

content in the matrix of IMI 834–SM1140 + would also be expected to reduce matrix ductility [22]. A reduction in ductility coupled with an increase in microhardness will increase the propensity of the matrix to crack and may be contributory factors in the transgranular matrix cleavage observed in this MMC.

4. Conclusions

1. Interfacial reaction is greater in IMI 834 MMCs than in Ti–6Al–4V MMCs, because of the higher consolidation temperature.

2. The microstructure of the foil-bonded alloys and MMC matrices is not the optimum in terms of mechanical properties as a result of the thermal history of the fibre–foil process.

3. MMCs reinforced with SM1240 fibre exhibit stringers of boron precipitates along foil bond lines. This is a result of boron diffusion from the fibre coating during consolidation.

4. A FPM of 7.1 produces MMCs of (Ti–6Al–4V) –SM1240 with excellent microstructural quality, exhibiting minimal matrix and interfacial cracking, no longitudinal fibre bending and few touching fibres.

5. The larger diameter of the SM1140 + fibre means that (Ti–6Al–4V)–SM1140+ requires a FPM of around 6.2 to produce acceptable microstructural quality.

6. The higher residual stresses inherent in IMI 834 MMCs cause matrix and interfacial damage to be present after fabrication at a FPM of 7.1. High numbers of touching fibres also result. Reducing the FPM to 6.3 alleviates these problems and results in a high-quality microstructure.

7. There is evidence that IMI 834–SM1140+ has a higher matrix carbon content than the other MMCs or foil-bonded alloys.

Acknowledgements

The authors gratefully acknowledge support from the Ministry of Defence Applied Research Programme, and from the Department of Trade and Industry CARAD (Civil Aviation Research and Development) programme.

References

1. Materials Strategy Commission Technology Foresight Programme, Draft Report on Aerospace Structural Materials (Institute of Materials, London, 1995).
2. Titanium Matrix Composite Turbine Engine Components Consortium, (TMCTECC), Promotional Brochure (United Technologies Corporation, Pratt & Whitney, FI).
3. J. G. ROBERTSON, NATO Advisory Group for Aerospace Research and Development, Neuilly-sur-Seine, Report 796 (1994) pp. 7. 1–7.8.
4. A. WOLFENDEN, K.D. HALL and B. A. LERCH, *J. Mater. Sci.* **31** (1996) 1489.
5. Z. X. GUO and B. DERBY, *J. Microsco.* **169** (1993) 269.
6. R. A. MACKAY, *Scripta Metall.* **24** (1990) 167.
7. S. MALL and P. G. ERMER, *J. Compos. Mater.* **25** (1991) 1668.
8. B. SANDERS and S. MALL, *Mater. Sci. Engng.* **A200** (1995) 130.
9. M. J. DONACHIE, in "Titanium: a technical guide" (American Society for Metals, Metals Park, OH, 1988) pp. 29–34.
10. A. K. CHAKRABARTI, M. BURN, D. FOURNIER and G. W. KUHLMAN, in Proceedings of the Sixth World Conference on Titanium, Vol. II, edited by P. Lacombe, R. Tricot and G. Beranger (Les Editions De Physique, Les Ulis, 1988) pp. 1339–1344.
11. X. DEMULSANT and J. MENDEZ, *Fatique Fract. Engng Mater. & Struct.* **18** (1995) 1483.
12. R. I. JAFFEE, L. WAGNER and G. LUTTJERING, in Proceedings of the Sixth World Conference on Titanium, Vol. II, edited by P. Lacombe, R. Tricot and G. Beranger (Les Editions De Physique, Les Ulis, 1988) pp. 1501–1506.
13. L. WAGNER and G. LURJERING, in Proceedings of the Sixth World Conference on Titanium, Vol. II, edited by P. Lacombe, R. Tricot and G. Beranger (Les Editions De Physique, Les Ulis, 1988) pp. 345–350.
14. N. LEGRAND, J. GRISON and L. REMY, in "Fatigue 96", Proceedings of the Sixth International Fatigue Congress Vol. III, edited by G. Lutjering and H. Nowack (Pergamon, Oxford, 1996) pp. 1451–1456.
15. S. V. SWEBY, A. L. DOWSON and P. BOWEN, 1996 TMS Annual Meeting, Anaheim, CA, 5–8 February 1996.
16. P. D. NICOLAOU, H. R. PIEHLER and M. A. KUHNI, in "Developments in ceramic and metal-matrix composites", edited by K. Upadhya (Minerals, Metals and Materials Society, Pennsylvania, PA, 1991) pp. 37–47.
17. T. P. GABB, J. GAYDA and R. A. MACKAY, *J. Compos. Mater.* **24** (1990) 667.
18. B. A. LERCH, D. R. HULL and T. A. LEONHARDT, Lewis Research Center, National Aeronautics and Space Administration, Cleveland, OH, Technical Memorandum 100938 (1988).
19. C. J. SMITHELLS "Metals reference book" (Butterworth, London, 5th Edn, 1976).
20. T. ASKILL, in "Tracer diffusion data for metals, alloys and simple oxides" (Plenum, London, 1970) p. 52.
21. R. NASLAIN, J. THEBAULT and R. PAILLER in Proceedings of the 1975 International Conference on Composite Materials, Vol. I (Metallurgical Society of AIME, New York, 1976) pp. 116–136.
22. A. D. McQUILLAN and M. K. McQUILLAN, in "Metallurgy of the rarer metals—4: Titanium" (Butterworth, London, 1956) pp. 182–189, 340.
23. V. A. LIKHACHEV, Y. D. KHESIN, O. S. BELOVA, I. N. ANDRONOV and G. V. MEDVEDEVA, *Fiz. Metall. Metalloved.* **47** (1979) 834–842.
24. C. F. YOLTON and J. H. MOLL, in "Titanium ^{2}95: Science and technology", edited by P. A. Blenkinsop, W. J. Evans and H. M. Flower (Institute of Materials, London, 1996) pp. 2755–2762.
25. D. A. PORTER and K. E. EASTERLING, in "Phase transformations in metals and alloys" (Van Nostrand Reinhold, New York, 1988) pp. 92–102.
26. M. P. THOMAS, S. F. BATE, J. G. ROBERTSON and M. R. WINSTONE, *Mater. Sci. Technol.* (1998) in press.
27. D. F. NEAL in "Titanium: Science and technology", Vol. 4, edited by G. Lutjering, U. Zwicker and W. Bunk (Deutsche Gesellschaft für Metallkunde EV, Oberursel, 1985) pp. 2419–2424.
28. H. RENNER, H. KESTLER and H. MUGHRABI, in "Fatigue '96", Proceedings of the Sixth International Fatigue Congress, Vol. II, edited by G. Lutjering and H. Nowack (Pergamon, Oxford, 1996) pp. 935–940.
29. D. F. NEAL and S. P. FOX in "Titanium '92: Science and technology", edited by F. H. Froes and I. Caplan (Minerals, Metals and Materials Society, Pennsylvania, PA, 1993) pp. 287–294.
30. W. T. DONLON, J. E. ALLISON and J. V. LASECKI, in "Titanium '92: Science and technology", edited by F. H. Froes and I. Caplan (Minerals, Metals and Materials Society, Pennsylvania, PA, 1993) pp. 295–302.

31. A. P. WOODFIELD, M. H. LORETTO and R. E. SMALLMAN, in "Titanium: Science and technology", Vol. 3, edited by G. Lutjering, U. Zwicker and W. Bunk (Deutsche Gesellschaft für Metallkunde EV, Obseursel, 1985) pp. 1527–1534.
32. L. HAZELL, Unpublished results, CSMA Ltd, Manchester, (September 1994).
33. J. F. DURODOLA and C. RUIZ, in "Advanced composites '93", edited by T. Chandra and A. K. Dhingra (Minerals, Metals and Materials Society, Pennsylvania, PA, 1993) pp. 1133–1139.
34. J. H. TWEED, J. COOK, N. L. HANCOX, R. J. LEE and R. F. PRESTON, NATO Advisory Group for Aerospace Research and Development, Neuilly-sur-Seine, Report 796 (1994) pp. 20.1–20.10.

Received 19 June 1997
and accepted 11 May 1998